

Quasinormal modes and dispersion relations for quarkonium in a plasma

Nelson R. F. Braga^a and Luiz F. Ferreira^a

^a*Instituto de Física, Universidade Federal do Rio de Janeiro, Caixa Postal 68528, RJ 21941-972 – Brazil*

E-mail: braga@if.ufrj.br, luizfaulhaber@if.ufrj.br

ABSTRACT: Recent investigations show that the thermal spectral function of heavy $b\bar{b}$ and $c\bar{c}$ vector mesons can be described using holography. These studies consider a bottom up model that captures the heavy flavour spectroscopy of masses and decay constants in the vacuum and is consistently extended to finite temperature. The corresponding spectral functions provide a picture of the dissociation process in terms of the decrease of the quasi-state peaks with temperature.

Another related tool that provides important information about the thermal behaviour is the analysis of the quasinormal modes. They are field solutions in a curved background assumed to represent, in gauge/gravity duality, quasi-particle states in a thermal medium. The associated complex frequencies are related to the thermal mass and width. We present here the calculation of quasinormal modes for charmonium and bottomonium using the holographic approach. The temperature dependence of mass and thermal width are investigated. Solutions corresponding to heavy mesons moving into the plasma are also studied. They provide the dependence of the real and imaginary parts of the frequency with the quasi-particle momenta, the so called dispersion relations.

KEYWORDS: Gauge-gravity correspondence, Phenomenological Models

Contents

1	Introduction	1
2	Holographic model for heavy vector mesons	2
3	Thermal spectral function	5
3.1	Equations of motion	5
3.2	Retarded Green's function	6
3.3	Spectral Function	7
3.4	Numerical Results	8
4	Quasinormal modes	9
4.1	Quasi-particles at rest in the medium	13
4.2	Quasi-Particles in motion: dispersion relations	14
5	Discussions of the results and Conclusions	15
6	Appendix	18

1 Introduction

The fraction of heavy vector mesons produced in a heavy ion collision provides important information about the possible formation of a quark gluon plasma[1, 2]. This is so because the presence of a thermal medium leads to the partial dissociation of these hadronic states. That is why it is important to understand the thermal behaviour of heavy mesons. In particular, the dependence of the dissociation degree on the temperature of the medium and on the state of motion of the meson.

The thermal behaviour of heavy vector mesons can be described using holographic bottom up models. A holographic model for $b\bar{b}$ (bottomonium) and $c\bar{c}$ (charmonium), involving two dimensionfull parameters, was proposed in Refs. [3–5]. An improved model containing three energy parameters appeared then in Refs. [6, 7]. These parameters have a simple physical interpretation. They represent: the quark mass and the string tension, that are related to the mass spectra, and an ultraviolet (UV) energy scale, necessary in order to fit the decay constant spectra. This UV energy parameter is related to the large mass change that occurs in a non hadronic decay, when a heavy vector meson transforms into light leptons.

The thermal spectral function for heavy vector mesons was constructed using this holographic approach in references [6, 7]. Quasi-Particle states appear as peaks that broadens when the temperature increases.

Important information about the behaviour of hadrons inside a thermal medium can be obtained also from the so called quasinormal modes. They are gravitational field solutions that play the role of gravity duals to quasi-particle states. The associated frequencies are complex and the imaginary parts are related to the thermal width of the quasi-state. Quasinormal modes are the finite temperature version of the normalized solutions, that describe particle states at zero temperature in holography.

We will develop here the calculation of quasinormal modes using the bottom up holographic model of references [6, 7]. The dependence of the real and imaginary part of the frequency on the temperature will be investigated for charmonium and bottomonium states. Then the dispersion relations will be considered. The dependence of the complex frequencies on the linear momentum, for hadrons moving inside a plasma, will be analysed for different temperatures. This type of analysis provides a detailed picture of the thermal behaviour of the heavy vector mesons in a medium like the quark gluon plasma.

The article is organized in the following way. In section **2** we review the holographic model for charmonium and bottomonium. Then in section **3** we study the spectral functions for charmonium and bottomonium. The quasinormal modes are calculated in section **4** and conclusions and final comments are shown in section **5**.

2 Holographic model for heavy vector mesons

The bottom up holographic models for heavy vector mesons of refs. [6, 7] are defined, in the zero temperature case, in 5-d anti-de Sitter space-time, with metric

$$ds^2 = \frac{R^2}{z^2}(-dt^2 + d\vec{x} \cdot d\vec{x} + dz^2). \quad (2.1)$$

The gravity duals of heavy vector mesons are fields $V_m = (V_\mu, V_z)$ ($\mu = 0, 1, 2, 3$), that are assumed to represent the gauge theory currents $J^\mu = \bar{\psi}\gamma^\mu\psi$. The action integral is:

$$I = \int d^4x dz \sqrt{-g} e^{-\phi(z)} \left\{ -\frac{1}{4g_5^2} F_{mn} F^{mn} \right\}, \quad (2.2)$$

where $F_{mn} = \partial_m V_n - \partial_n V_m$. The energy parameters are introduced through the background scalar field $\phi(z)$. The scalar field used in ref.[6]

$$\phi(z) = k^2 z^2 + \tanh\left(\frac{1}{Mz} - \frac{k}{\sqrt{\Gamma}}\right), \quad (2.3)$$

was usefull for charmonium states but did not provide a nice phenomenological description of the spectra of decay constants and masses for bottomonium. The improved version, presented in ref. [7], that we will use here, provides a nice fit for both chamonium and bottomonium states. It has the following form:

$$\phi(z) = k^2 z^2 + Mz + \tanh\left(\frac{1}{Mz} - \frac{k}{\sqrt{\Gamma}}\right). \quad (2.4)$$

The parameters k and Γ have simple interpretations in terms of just the mass spectra of mesons made up of two heavy quarks: k is related to the quark mass while Γ , with dimension of energy squared, is related to the string tension of the strong quark anti-quark interaction. On the other hand, the third parameter M has a more subtle interpretation. Heavy vector mesons undergo non hadronic decay processes, when the final state consists of light leptons. In such transitions, that are not governed by the strong interaction, there is a very large mass change. The parameter M is representing effectively the mass scale of such a transition, characterized by a matrix element of the form $\langle 0 | J_\mu(0) | n \rangle = \epsilon_\mu f_n m_n$, representing a transition from a meson at radial excitation level n to the hadronic vacuum. The decay constant f_n is essentially proportional to this matrix element and the large mass parameter M makes it possible to fit the corresponding spectra.

The simplest way to realise gauge gravity duality is to gauge away the z component: $V_z = 0$. Then the remaining V_μ work as sources for the currents J^μ . The equation of motion for the $\mu = (1, 2, 3)$ components, denoted here generically as V , in momentum space reads

$$\partial_z \left[\frac{R}{z} e^{-\phi(z)} \partial_z V(p, z) \right] - p^2 \frac{R}{z} e^{-\phi(z)} V(p, z) = 0. \quad (2.5)$$

The normalizability requirement for solutions of equation of motion (2.5) corresponds to the boundary condition $V(p, z = 0) = 0$. The corresponding solutions $V(p, z) = \Psi_n(z)$ show up for a discrete spectrum of $p^2 = -m_n^2$ where m_n are interpreted as the masses of the corresponding meson states.

Decay constants are proportional to the transition matrix from the vector meson n excited state to the vacuum: $\langle 0 | J_\mu(0) | n \rangle = \epsilon_\mu f_n m_n$. In the present holographic model they are given by [6]

$$f_n = \frac{1}{g_5 m_n} \lim_{z \rightarrow 0} \left(\frac{R}{z} e^{-\phi(z)} \partial_z \Psi_n(z) \right). \quad (2.6)$$

The values of the parameters that describe charmonium and bottomonium are respectively:

$$k_c = 1.2 \text{ GeV}; \quad \sqrt{\Gamma_c} = 0.55 \text{ GeV}; \quad M_c = 2.2 \text{ GeV}; \quad (2.7)$$

$$k_b = 2.45 \text{ GeV}; \quad \sqrt{\Gamma_b} = 1.55 \text{ GeV}; \quad M_b = 6.2 \text{ GeV}. \quad (2.8)$$

We show on Tables 1 and 2 the results for charmonium and bottomonium, calculated in ref. [7] using this model. For comparison we shown inside parentheses the corresponding available experimental data. The masses come directly from [8] while decay constants are obtained from the experimental values of masses and electron positron decay widths $\Gamma_{V \rightarrow e^+ e^-}$ using the relation [9]:

$$f_V^2 = \frac{3m_V \Gamma_{V \rightarrow e^+ e^-}}{4\pi \alpha^2 c_V}, \quad (2.9)$$

Holographic (and experimental) results for bottomonium		
State	Mass (MeV)	Decay constants (MeV)
1S	6905 (9460.30 \pm 0.26)	719 (715.0 \pm 2.4)
2S	8871 (10023.26 \pm 0.32)	521 (497.4 \pm 2.2)
3S	10442 (10355.2 \pm 0.5)	427 (430.1 \pm 1.9)
4S	11772 (10579.4 \pm 1.2)	375 (340.7 \pm 9.1)

Table 1. Holographic masses and decay constants for the bottomonium S -wave resonances. Experimental values inside parentheses for comparison.

Holographic (and experimental) results for charmonium		
State	Mass (MeV)	Decay constants (MeV)
1S	2943 (3096.916 \pm 0.011)	399 (416 \pm 5.3)
2S	3959 (3686.109 \pm 0.012)	255 (296.1 \pm 2.5)
3S	4757 (4039 \pm 1)	198 (187.1 \pm 7.6)
4S	5426 (4421 \pm 4)	169 (160.8 \pm 9.7)

Table 2. Holographic masses and decay constants for the charmonium S -wave resonances. Experimental values inside parentheses for comparison.

where $\alpha = 1/137$ and the charge coefficients c_v for the two families that we consider are $c_{c\bar{c}} = 4/9$ and $c_{b\bar{b}} = 1/9$. Decay constants obtained from experimental data decrease monotonically with the radial excitation level for both charmonium and bottomonium states. It is important to note the very nice fit of the decay constants provided by the model compared with those obtained from experimental data. This was the main motivation for the construction of this alternative approach to the holographic description of heavy vector mesons. Holographic models provide in general results that are not compatible with the experimental data regarding decay constants. For example, the hard wall model, proposed in refs. [10–12], provides decay constants that increase with the radial excitation number, while the soft wall model [13] leads to decay constants that are degenerate with respect to the radial excitation level.

Now, one could ask: why is it important to have a nice fit for the zero temperature decay constants when one aims to find an appropriate description of the finite temperature thermal behavior? It is simple to understand this fact, once we remind us about the connection between decay constants and the spectral function.

The thermal spectral function is the imaginary part of the retarded Green’s function. The relevant part of the Green’s function is the two point function that, at zero temperature, has a spectral decomposition in terms of masses m_n and decay constants f_n of the states:

$$\Pi(p^2) = \sum_{n=1}^{\infty} \frac{f_n^2}{(-p^2) - m_n^2 + i\epsilon}. \quad (2.10)$$

The imaginary part of eq.(2.10) is a sum of delta peaks with coefficients proportional to the square of the decay constants: $f_n^2 \delta(-p^2 - m_n^2)$. At finite temperature, the quasi-particle

states appear in the spectral function as broader peaks as the temperature T of the medium increase. This analysis strongly suggests that a consistent extension of a hadronic model to finite temperature should take into account the zero temperature behavior, where decay constants play an essential role.

The extension to finite temperature is obtained by replacing the AdS space of eq. (2.1) by an AdS black hole geometry

$$ds^2 = \frac{R^2}{z^2} \left(-f(z)dt^2 + d\vec{x} \cdot d\vec{x} + \frac{dz^2}{f(z)} \right), \quad (2.11)$$

with $f(z) = 1 - \frac{z^4}{z_h^4}$, where z_h is the horizon position. The black hole temperature comes from the requirement of absence of a conical singularity at the horizon, in the Euclidean version of the metric. In this imaginary time formulation, the time variable is periodic, with period $0 \leq t \leq \beta = 1/T$, where T is the temperature. The regularity of the metric leads to

$$T = \frac{|f'(z)|_{(z=z_h)}}{4\pi} = \frac{1}{\pi z_h}. \quad (2.12)$$

3 Thermal spectral function

3.1 Equations of motion

The equations of motion for the holographic model come from action (2.2) with the metric (2.11). One chooses again the radial gauge $V_z = 0$ and consider plane wave solutions of the form: $V_\mu(z, x_1, x_2, x_3, t) = e^{-\omega t + i q x_3} V_\mu(z, \omega, q)$ propagating in the x_3 direction with the wave vector $p_\mu = (-\omega, 0, 0, q)$. The equations have the following form

$$V_t'' - \left(\frac{1}{z} + \phi' \right) V_t' - \frac{q}{f} (qV_t + \omega V_3) = 0, \quad (3.1)$$

$$V_\beta'' + \left(\frac{f'}{f} - \frac{1}{z} - \phi' \right) V_\beta' + \frac{1}{f^2} (\omega^2 - q^2 f) V_\beta = 0, \quad (\beta = 1, 2) \quad (3.2)$$

$$V_3'' + \left(\frac{f'}{f} - \frac{1}{z} - \phi' \right) V_3' + \frac{\omega}{f^2} (qV_t + \omega V_3) = 0, \quad (3.3)$$

$$\omega V_t' + q f V_3' = 0 \quad (3.4)$$

where the prime ($'$) denotes the derivative with respect to z . The corresponding equations in terms of the electric field components: $E_1 = \omega V_1$, $E_2 = \omega V_2$ and $E_3 = \omega V_3 + qV_t$, are given by

$$E_\alpha'' + \left(\frac{f'}{f} - \frac{1}{z} - \phi' \right) E_\alpha' + \frac{\omega^2 - q^2 f}{f^2} E_\alpha = 0, \quad (\alpha = 1, 2) \quad (3.5)$$

$$E_3'' + \left(\frac{\omega^2}{\omega^2 - q^2 f} \frac{f'}{f} - \frac{1}{z} - \phi' \right) E_3' + \frac{\omega^2 - q^2 f}{f^2} E_3 = 0. \quad (3.6)$$

3.2 Retarded Green's function

In the four dimensional vector gauge theory we define a retarded Green's functions of the currents J_ν as

$$G_{\mu\nu}^R(p) = -i \int d^4x e^{-ip \cdot x} \theta(t) \langle [J_\mu(x), J_\nu(0)] \rangle. \quad (3.7)$$

Current conservation implies that $p^\mu G_{\mu\nu}^R(p) = 0$. So, the structure of the Greens function at zero temperature can be written in terms of a projector that makes explicit this property:

$$G_{\mu\nu}^R(p) = P_{\mu\nu} \Pi(p^2), \quad (3.8)$$

where

$$P_{\mu\nu} = \eta_{\mu\nu} - \frac{p_\mu p_\nu}{p^2}. \quad (3.9)$$

At finite temperature, in thermal equilibrium, it is interesting to separate this projector into transverse and longitudinal parts [17] introducing

$$\begin{aligned} P_{00}^T &= 0, & P_{0i}^T &= 0, & P_{ij}^T &= \delta_{ij} - \frac{p_i p_j}{\mathbf{p}^2} \\ P_{\mu\nu}^L &= P_{\mu\nu} - P_{\mu\nu}^T. \end{aligned} \quad (3.10)$$

Then the retarded Green's function can be written in the finite temperature case when there is rotation invariance as

$$G_{\mu\nu}^R(p) = P_{\mu\nu}^T \Pi^T(p_0, \mathbf{p}^2) + P_{\mu\nu}^L \Pi^L(p_0, \mathbf{p}^2), \quad (3.11)$$

where $\Pi^T(p_0, \mathbf{p}^2)$ and $\Pi^L(p_0, \mathbf{p}^2)$ are independent scalar functions.

Choosing, as in the previous section, the wave vector with the form $p_\mu = (-\omega, 0, 0, q)$, corresponding to propagation in the z direction, the relevant (non-vanishing) components of the Green's function can all be written in terms of the longitudinal and transversal scalar functions

$$G_{11}^R(p) = G_{22}^R = \Pi^T(\omega, q), \quad G_{33}^R(p) = \frac{\omega^2}{\omega^2 - q^2} \Pi^L(\omega, q), \quad (3.12)$$

$$G_{tt}^R(p) = \frac{q^2}{\omega^2 - q^2} \Pi^L(\omega, q), \quad G_{t3}^R(p) = -\frac{q\omega}{\omega^2 - q^2} \Pi^L(\omega, q). \quad (3.13)$$

Considering now the holographic approach, the gauge theory current correlators are represented in terms of the vector fields living in the five dimensional space and described by the

action integral of eq. (2.2) with metric (2.11). In momentum space the on shell action takes the form

$$S = \frac{R}{2g_5^2} \int \frac{d\omega dq}{(2\pi)^2} \left[\frac{e^{-\phi}}{z} \left\{ V_t(z, -p) \partial_z V_t(z, p) - f \mathbf{V}(z, -p) \cdot \partial_z \mathbf{V}(z, p) \right\} \right]_0^{z_h}. \quad (3.14)$$

It is convenient to express this action in terms of the electric field components

$$S = -\frac{R}{2g_5^2} \int \frac{d\omega dq}{(2\pi)^2} \left[\frac{e^{-\phi}}{z} \frac{f}{\omega^2} \sum_{j=1}^3 \left(1 - \frac{q^2}{\omega^2} f \right)^{-\delta_{j3}} E_j(z, -p) \partial_z E_j(z, p) \right]. \quad (3.15)$$

The z dependent part of the field, the so called bulk to boundary propagator, can be separated from the boundary value E_j^0 as

$$E_j^{(-)}(z, p) = \mathcal{E}_j(z, p) E_j^0(p), \quad (j = 1, 2, 3) \quad (3.16)$$

where the functions $\mathcal{E}_j(z, p)$ are defined to satisfy $\mathcal{E}_j(0, p) = 1$ and the superscript $(-)$ indicates that $E_j^{(-)}(z, p)$ satisfies the infalling condition at the horizon, as required by the Lorentzian form of Son-Starinets prescription [15]. Then, substituting (3.16) in the action (3.15) one finds

$$S = -\frac{R}{2g_5^2} \int \frac{d\omega dq}{(2\pi)^2} \left[\frac{e^{-\phi}}{z} \frac{f}{\omega^2} \sum_{j=1}^3 \left(1 - \frac{q^2}{\omega^2} f \right)^{-\delta_{j3}} E_j^0(-p) \mathcal{E}_j(z, p) \partial_z \mathcal{E}_j(z, p) E_j^0(p) \right]_0^{z_h} \quad (3.17)$$

In terms of the boundary values of the potential this action reads

$$S = \frac{R}{2g_5^2} \int \frac{d\omega dq}{(2\pi)^2} \left[\frac{e^{-\phi}}{z} f \left(\frac{\omega^2}{\omega^2 - q^2 f} \left\{ V_3^0(-p) V_3^0(p) + \frac{q}{\omega} V_3^0(-p) V_t^0(-p) - \frac{q}{\omega} V_t^0(-p) V_3^0(-p) \right. \right. \right. \\ \left. \left. \left. + \frac{q^2}{\omega^2} V_t^0(-p) V_t^0(p) \right\} \mathcal{E}_3(z, -p) \partial_z \mathcal{E}_3(z, p) + \sum_{\alpha=1}^2 V_\alpha^0(-p) V_\alpha^0(p) \mathcal{E}_\alpha(z, -p) \partial_z \mathcal{E}_\alpha(z, p) \right) \right]_0^{z_h} \quad (3.18)$$

Finally, using the Son-Starinets [15] prescription for the vector field case one finds

$$\frac{G_{tt}^R}{q^2} = -\frac{G_{tx_3}^R}{q\omega} = -\frac{G_{3t}^R}{q\omega} = \frac{G_{33}^R}{\omega^2} = -\frac{R}{g_5^2} \frac{1}{\omega^2 - q^2} \lim_{z \rightarrow 0} \frac{f e^{-\phi}}{z} \partial_z \mathcal{E}_3(z, p) \\ G_{11}^R = -\frac{R}{g_5^2} \lim_{z \rightarrow 0} \frac{f e^{-\phi}}{z} \partial_z \mathcal{E}_1(z, p), \quad G_{22}^R = -\frac{R}{g_5^2} \lim_{z \rightarrow 0} \frac{f e^{-\phi}}{z} \partial_z \mathcal{E}_2(z, p). \quad (3.19)$$

3.3 Spectral Function

In order to calculate the spectral function it is convenient write the equations of motion for the electric fields (3.5) and (3.6) in terms of the bulk to boundary propagator $E_j(z, p) = \mathcal{E}_j(z, p) E_j^0(p)$,

$$\partial_z^2 \mathcal{E}_\alpha + \left(\frac{\partial_z f}{f} - \frac{1}{z} - \partial_z \phi \right) \partial_z \mathcal{E}_\alpha + \frac{\omega^2 - q^2 f}{f^2} \mathcal{E}_\alpha = 0, \quad (\alpha = 1, 2) \quad (3.20)$$

$$\partial_z^2 \mathcal{E}_3 + \left(\frac{\omega^2}{\omega^2 - q^2 f} \frac{\partial_z f}{f} - \frac{1}{z} - \partial_z \phi \right) \partial_z \mathcal{E} + \frac{\omega^2 - q^2 f}{f^2} \mathcal{E}_3 = 0, \quad (3.21)$$

Now the spectral function can be extracted using the relation (3.19) presented in the last section. Particularly, in the case of $G_{x_3 x_3}^R$ and $G_{\alpha\alpha}^R$, the corresponding spectral functions in terms of the function \mathcal{E}_j are

$$\rho_{33}(\omega, q) \equiv -2\text{Im}G_{33}^R(\omega, q) = \frac{2R}{g_5^2} \frac{\omega^2}{\omega^2 - q^2} \lim_{z \rightarrow 0} \frac{f e^{-\phi}}{z} \partial_z \mathcal{E}_3(z, p), \quad (3.22)$$

$$\rho_{\alpha\alpha}(\omega, q) \equiv -2\text{Im}G_{\alpha\alpha}^R(\omega, q) = -\frac{2R}{g_5^2} \lim_{z \rightarrow 0} \frac{f e^{-\phi}}{z} \partial_z \mathcal{E}_\alpha(z, p), \quad (3.23)$$

where \mathcal{E} is the solution of the eqs. (3.20) and (3.21) satisfying the infalling boundary condition

$$\mathcal{E}(z \rightarrow z_h, \omega) \longrightarrow \left(1 - \frac{z}{z_h}\right)^{-i\omega/4\pi T} \left[1 + a_1 \left(1 - \frac{z}{z_h}\right) + a_2 \left(1 - \frac{z}{z_h}\right)^2 + \dots \right], \quad (3.24)$$

and the bulk to boundary condition

$$\mathcal{E}(z \rightarrow 0, \omega) = 1. \quad (3.25)$$

3.4 Numerical Results

We performed the numerical analysis of the spectral functions for the transverse and longitudinal sectors solving the equations (3.20) and (3.21), for the charmonium and bottomonium cases, using the boundary conditions (3.24),(3.25) for the fields. Then, relations (3.22) and (3.23) were used to find the spectral functions. The model parameters are the zero temperature ones, presented in section 2.

Let us start with the spectral functions for the vector mesons at rest. In this case the spectral function is the same for the transverse and longitudinal directions. In figure 1 we show the dissociation process at finite temperature for charmonium and in figure 2 the bottomonium case. Note that for both flavours the peaks broadens as the temperature increases. In particular, the peak broadens faster for charmonium than for bottomonium.

We also studied the spectral function at non vanishing momentum. In figure 3 and 4 the results obtained for charmonium and bottomonium, respectively, are shown at different value of momentum. In both cases one can observe the broadening that the height of the peaks in the longitudinal direction increase as the momentum increases while, for the transverse direction, the height of the peaks decrease. This can be interpreted as meaning that the quasiparticle states in longitudinal motion are more stable in the longitudinal than at rest ($q = 0$). On the other hand, quasiparticles in transverse motion are less stable than at rest. The localization of the peaks in terms of the frequencies change in both cases.

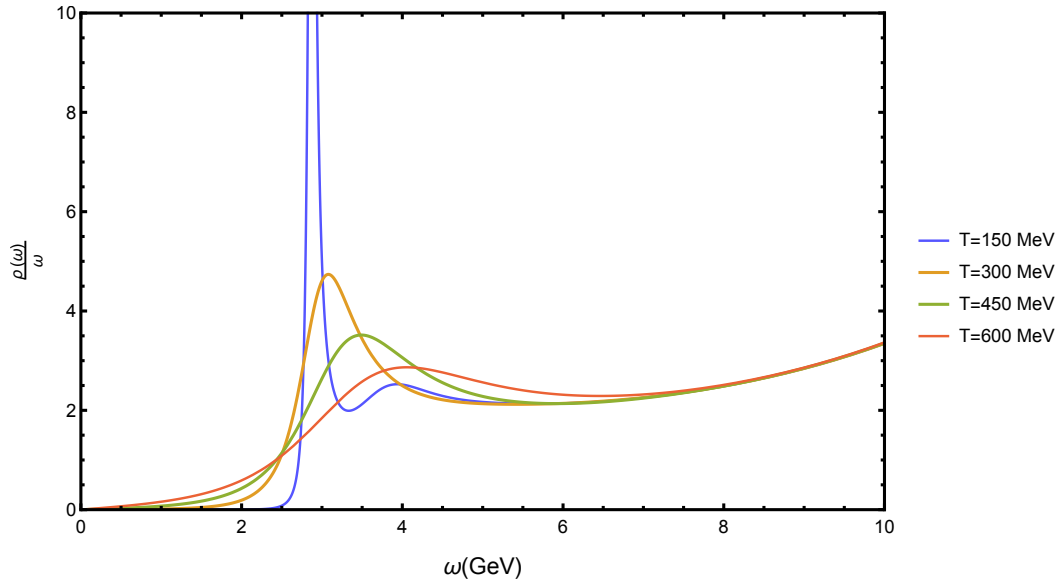


Figure 1. Spectral function for charmonium at rest for different values of temperature.

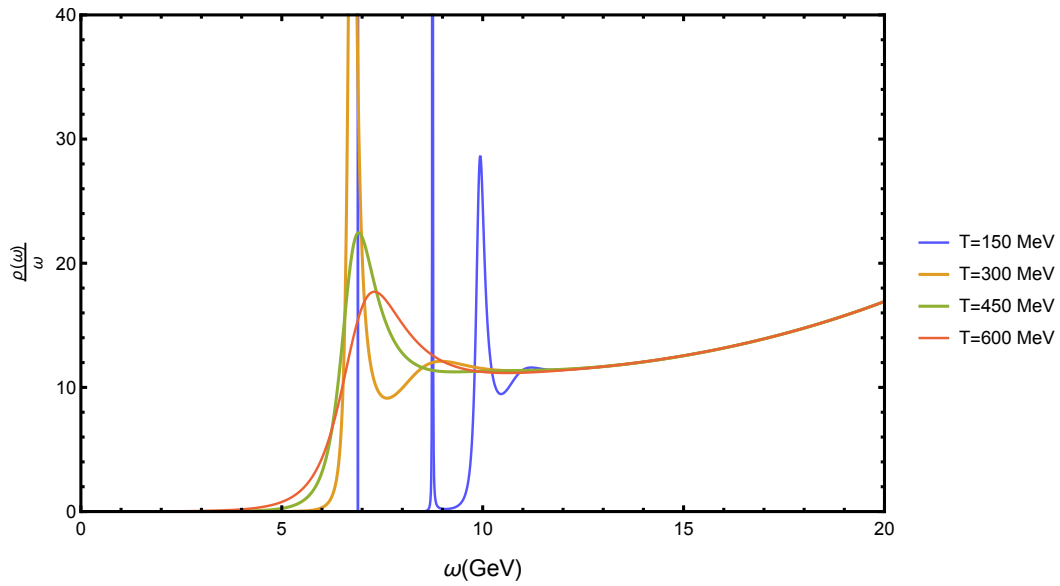


Figure 2. Spectral function for bottomonium at rest for different values of temperature.

4 Quasinormal modes

The peaks shown in figure 1 and 2 indicate that the corresponding retarded Green's functions present poles. These poles are related to the frequencies of the electromagnetic quasinormal

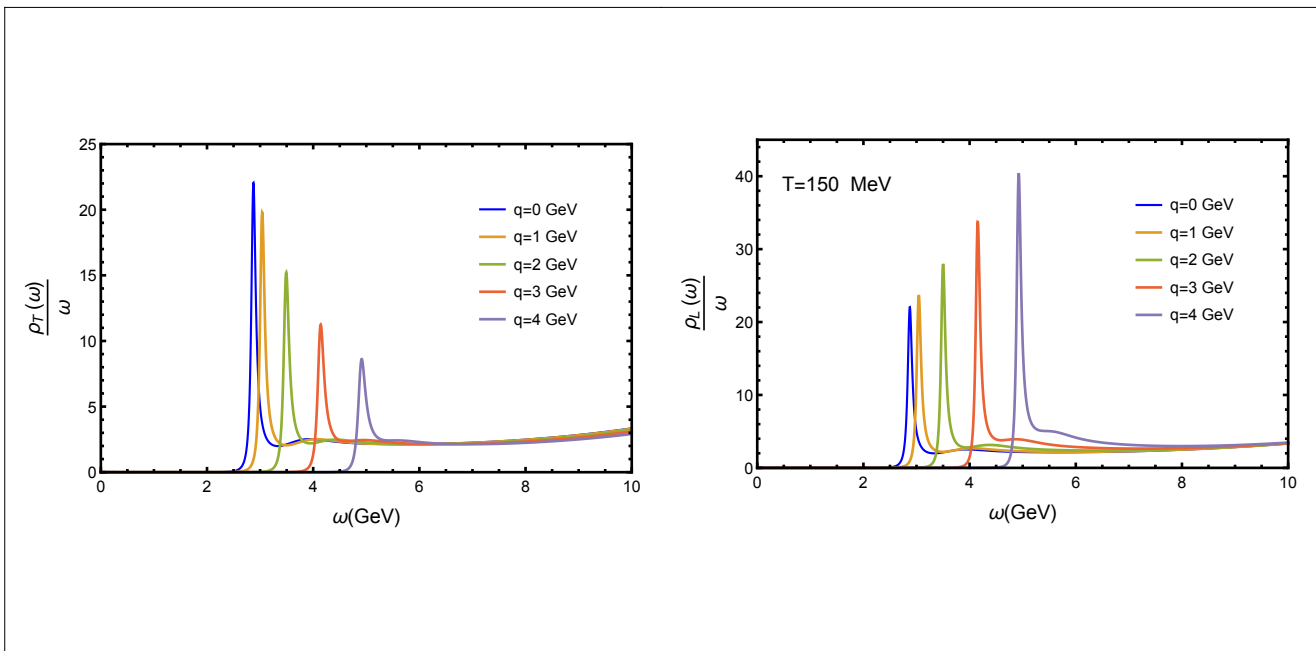


Figure 3. Spectral Function for charmonium with different values of linear momentum at fixed value of temperature.

modes of the black brane. The quasinormal modes correspond, in the dual gauge theory, to quasi-particle states of vector mesons. The frequencies of these quasinormal modes present real and imaginary parts, $\omega = \omega_R + i\omega_I$. The real part is related to the mass of the vector mesons when $q = 0$, while the imaginary part to the decay rate of the quasi-particle states formed near the confining/deconfining transition. One observes that when the temperature increases, the widths of the peaks increase and the mean life $\tau = 2\pi/\omega_I$ decrease.

In contrast to the zero temperature case, where there are particle states, represented by normalized solutions, in the finite temperature case we have quasi-particles, described by quasinormal modes. They are field solutions in the curved background, subject infalling condition at the horizon.

Previous studies of quasinormal modes in the context of gauge/gravity duality can be found, for example, in Refs. [14–25]. It is interesting to note that when one considers the conformal holographic AdS/CFT case, like in refs. [15, 17], there are no dimensionfull fixed parameters in the theory. So, at finite temperature, the only dimensionfull quantity is the temperature T . Then, for a quasi-particle with energy w and momentum q moving in the medium there are just two independent dimensionless quantities, usually taken as: $\mathbf{q} = q/T$ and $\mathbf{w} = w/T$. In particular, the authors of [17] show tables with the five lowest solutions for quasi-normal modes for different channels (field components) where one clearly sees that the general form of the real and imaginary parts of the mode solutions, for a fixed value of \mathbf{q}

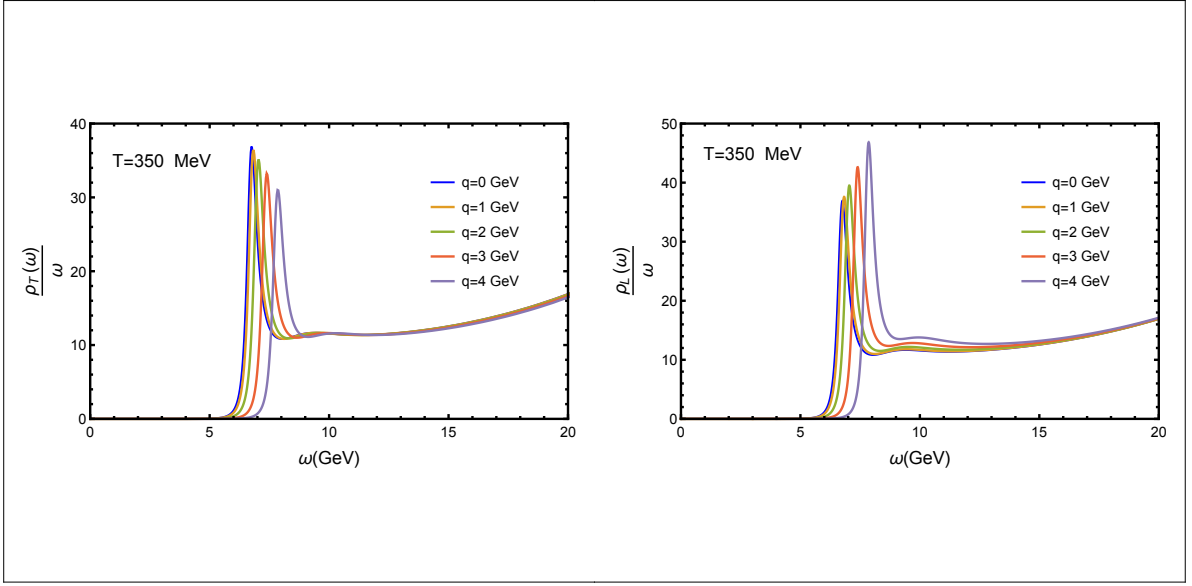


Figure 4. Spectral Function for bottomonium with different values of linear momentum at fixed value of temperature.

are of the form:

$$\Re(\mathfrak{w}) \equiv \frac{w_R}{T} = C_1; \Im(\mathfrak{w}) \equiv \frac{w_I}{T} = C_2, \quad (4.1)$$

where C_1 and C_2 are constants that depend on the channel and on the order of the mode. This means that the real and imaginary parts of the frequency w are just proportional to the temperature. At zero temperature, they vanish, since there are no mass parameters in the theory.

The situation is quite different in AdS/QCD models, where one introduces mass parameters, breaking conformal invariance. In these holographic models there is a non trivial dependence of the real and imaginary parts of the quasi-normal frequencies with the temperature. In particular, the real part w_R is related to the mass of the corresponding quasi-state and assumes, in the limit $T \rightarrow 0$, the value of the physical mass of the corresponding hadronic state in the vacuum. In the present case, the holographic model involves three energy parameters, that make it possible to fit the zero temperature masses and decay constants. The quasi-normal model solutions are rather non trivial and represent, as we will see in the sequence, the thermal behavior of the heavy vector mesons in the plasma. In order to have a deeper understanding about the effect of the introduction of the background $\phi(z)$ of eq. (2.4) we will discuss the hydrodynamic limit $\mathfrak{q} \ll 1$, $\mathfrak{w} \ll 1$ in the appendix.

We are going to obtain the quasinormal modes for electromagnetic perturbations by solving the equations of motion using numerical methods. The shooting method of refs. [26–30] is of particular interest for the present work since it is suited to find quasinormal modes

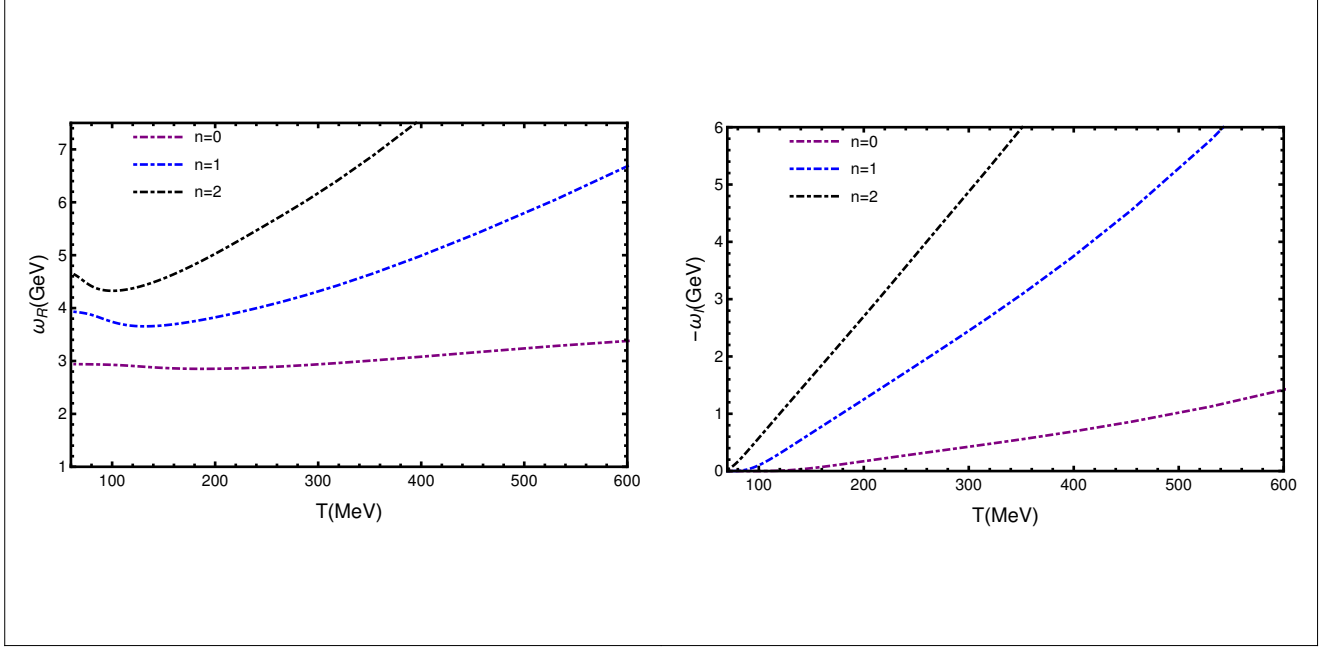


Figure 5. Real and imaginary parts of the frequencies of charmonium quasinormal modes as function of the temperature. The real part of the frequencies is shown on the left side, and the imaginary part on the right side.

of space-times that are only known numerically. The method consists in specifying two boundary conditions at the horizon, and then adjusting the free parameter given by the frequency. In our case we need to solve the equations (3.20) and (3.21)

$$\partial_z^2 \mathcal{E}_\alpha + \left(\frac{\partial_z f}{f} - \frac{1}{z} - \partial_z \phi \right) \partial_z \mathcal{E}_\alpha + \frac{\omega^2 - q^2 f}{f^2} \mathcal{E}_\alpha = 0, \quad (\alpha = 1, 2) \quad (4.2)$$

$$\partial_z^2 \mathcal{E}_3 + \left(\frac{\omega^2}{\omega^2 - q^2 f} \frac{\partial_z f}{f} - \frac{1}{z} - \partial_z \phi \right) \partial_z \mathcal{E}_3 + \frac{\omega^2 - q^2 f}{f^2} \mathcal{E}_3 = 0, \quad (4.3)$$

using the boundary conditions given by the infalling boundary conditions at the horizon position, presented in eq. (3.24),

$$\lim_{z \rightarrow z_h} \mathcal{E}_j(z, p) = \left(1 - \frac{z}{z_h} \right)^{-i\omega/4\pi T} \left[1 + a_1 \left(1 - \frac{z}{z_h} \right) + \dots \right]. \quad (4.4)$$

The second boundary condition is the derivative of the infalling condition :

$$\lim_{z \rightarrow z_h} \partial_z \mathcal{E}_j(z, p) = \left(1 - \frac{z}{z_h} \right)^{-i\omega/4\pi T} \left[\frac{-a_1}{z_h} + \frac{-a_2}{z_h} \left(1 - \frac{z}{z_h} \right) \dots \right]$$

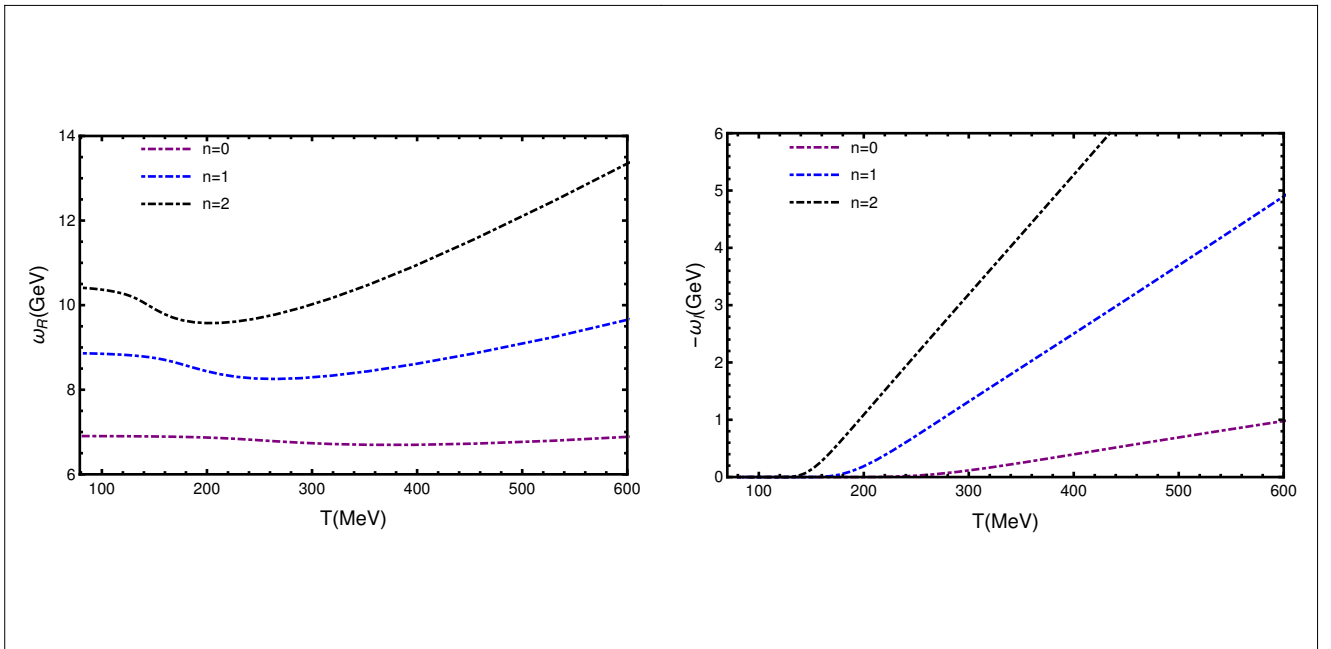


Figure 6. Real and imaginary parts of the frequencies of bottomonium quasinormal modes as function of the temperature. The real part of the frequencies is shown on the left side, and the imaginary part on the right side.

$$- \frac{i\omega}{(4\pi T)} \left(1 - \frac{z}{z_h}\right)^{-1} \lim_{z \rightarrow z_h} \mathcal{E}_j(z, p). \quad (4.5)$$

The coefficients that appear in the infalling condition can be determined inserting this condition into the equations of motions. Similarly to normal modes, the quasinormal modes exist only for a discrete set of frequencies ω_n .

In addition, it is necessary to ensure that the solution found by solving eqs. (4.2) and (4.3), using the boundary conditions at the horizon, is a quasinormal mode varying the frequency ω until the field satisfy the Dirichlet conditions at the boundary.

It is important to remark that in order to overcome the limitation of the shooting method when large imaginary part ω_I are present, it is necessary computing more coefficients of the near horizon expansion (4.4) for higher temperatures in order to find the quasinormal modes. This issue is discussed in [27].

4.1 Quasi-particles at rest in the medium

Using the shooting method the quasinormal frequencies were determined as a function of the temperature, for the case of zero momentum $q = 0$.

We show in figures 5 and 6 the results for the real and imaginary parts of the frequencies for the first three modes $n = 0, 1, 2$ with $q = 0$ for charmonium and bottomonium, respectively.

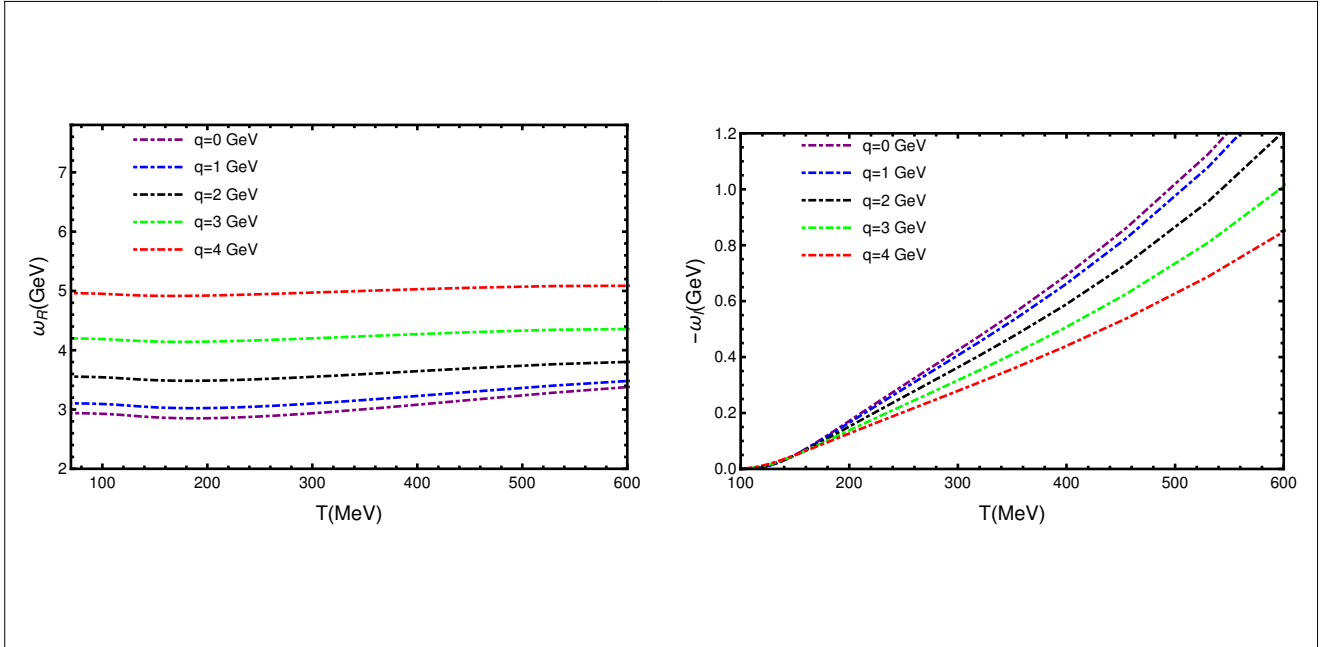


Figure 7. Numerical results for the quasinormal modes of the charmonium in the longitudinal direction as function of the temperature.

Note that the imaginary part of the frequency is negative and we show in our plots the values multiplied by minus one. From these figures one notes that in the region of high temperatures, the frequencies show a linear behaviour that is in agreement with ref.[17].

On the other hand, one can note that in the zero temperature limit, the real part of the quasinormal frequencies coincide with the corresponding mass spectrum of Table 1 and 2 and the behaviour at low temperature is not linear as in the high temperature. One also notes that the width for the charmonium grow faster than for bottomonium, showing that the dissociation process is more intense for charmonium.

4.2 Quasi-Particles in motion: dispersion relations

Longitudinal Perturbations

We found the quasinormal frequencies with finite momentum in the longitudinal sector using the shooting method in the equation (4.3). The variations of the quasinormal modes for different momentum as a function of the temperature for the ground state for charmonium and bottomonium are shown in Figs 7 and 8 respectively. As one can see, the real part of the frequencies increases with q . Such behaviour is consistent with the results in figures 3 and 4, where the position of the peaks of the spectral function shifts to high energies when the value of the momentum increases. A different thing happens with the imaginary part of the

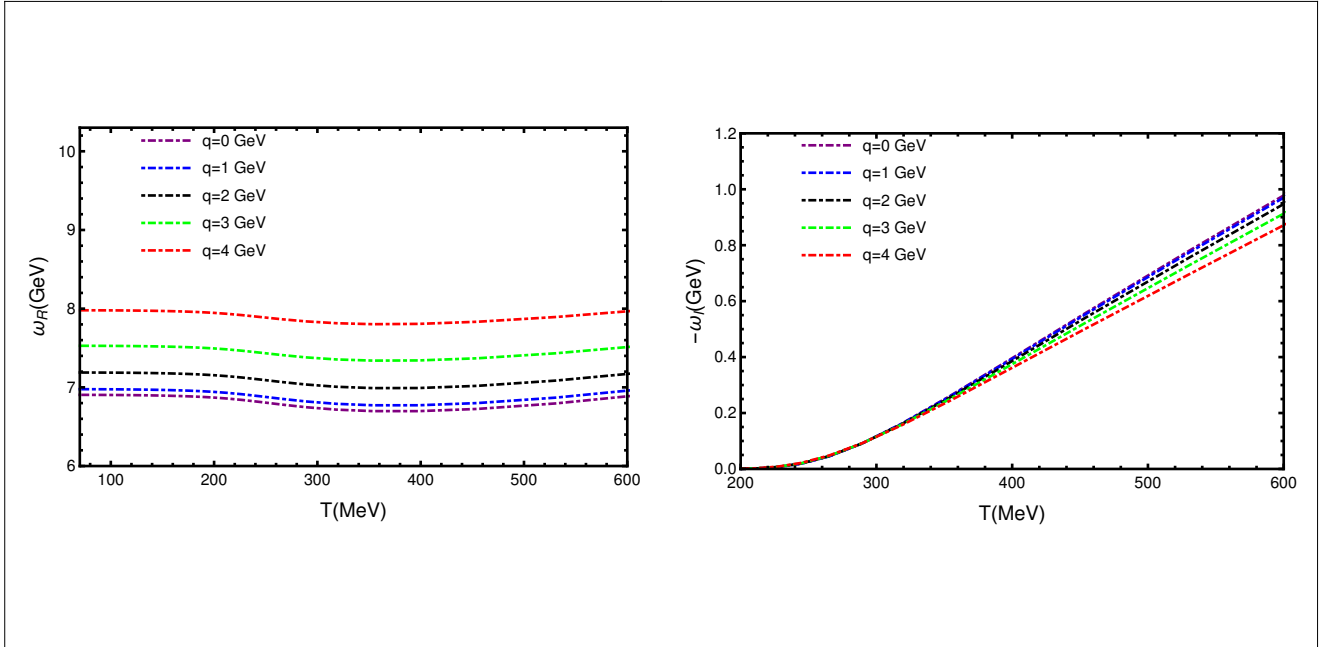


Figure 8. Numerical results for the quasinormal modes of the bottomonium in the longitudinal direction as function of the temperature.

frequencies (width of the peaks), which decreases with q as is shown in the right panel of the figures 7 and 8.

Transverse Perturbations

The results of the quasinormal modes for the transverse perturbations are presented in figures 9 and 10 as a function of the temperature. On one hand, the real part of the quasinormal frequencies have a similar behaviour to that of the longitudinal sector. On the other hand, the imaginary part of ω increases with momentum, in contrast to the longitudinal case. These results indicate that dissociation effect increases due to motion relative to the medium in the direction transverse to the polarization of the heavy vector mesons.

5 Discussions of the results and Conclusions

Using a holographic bottom up model, we have studied the real and imaginary parts of the quasinormal modes frequencies corresponding to charmonium and bottomonium states. The dependence with the temperature for quasi-particles at rest, or moving with respect to the medium, was investigated. For comparison, the spectral function for these heavy mesons was also obtained.

The outcomes from the quasinormal modes are consistent with the spectral function behaviour, as we now discuss. For mesons at rest, the real part of the frequency shows a

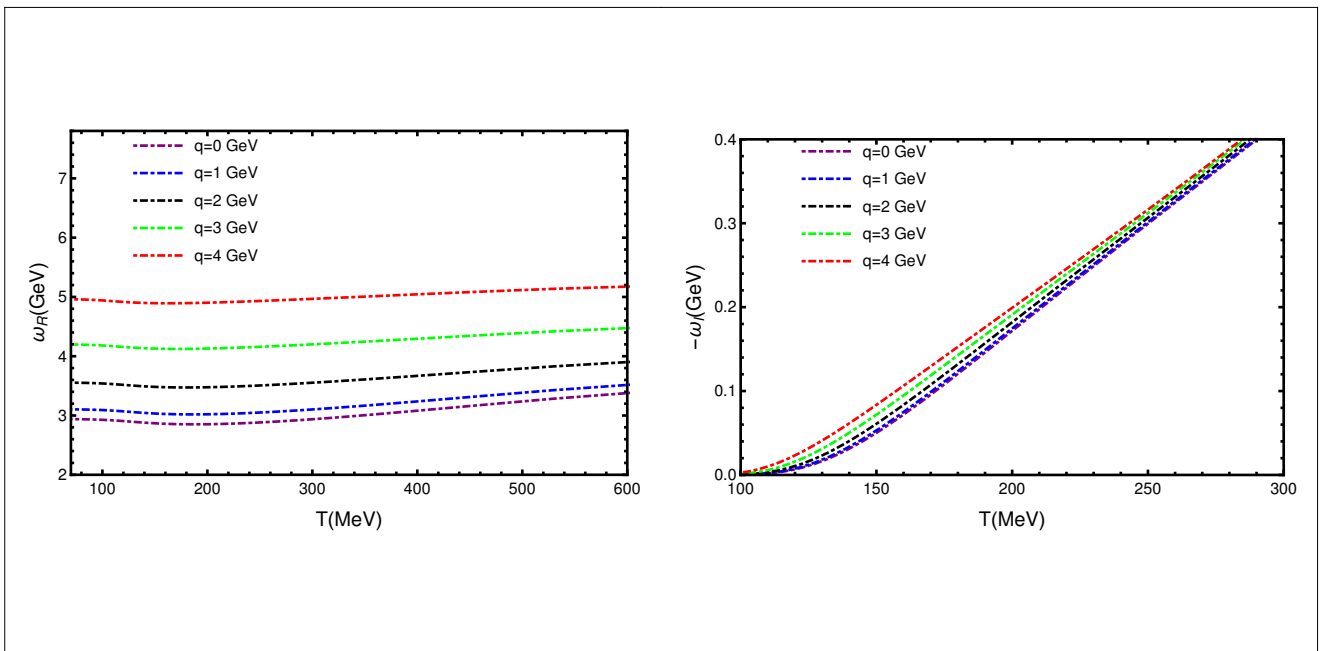


Figure 9. Numerical results for the quasinormal modes of the charmonium in the transverse direction as function of the temperature.

tendency to increase with the temperature. In terms of the spectral function this is translated into the increase in the position of the location of the peak. The imaginary part of the frequencies monotonically increase, a behaviour that is translated into the decrease in the height and an increase in the width of the peaks.

For mesons in motion with respect to the medium, the real part of the quasinormal modes frequencies increase with the value of the momentum, for both longitudinal and transverse motion. This is translated in terms of the spectral function into the increase in the value of the frequency where the peaks are located. For the imaginary part of the frequency, the behaviour is different if the motion is in the direction of the polarization (longitudinal case) or transverse to the polarization. In the longitudinal case the imaginary part decreases with the momentum. This behaviour is consistently reproduced in the spectral function as an increase in the height of the peaks. For transverse motion, the behaviour is the opposite. The imaginary part of the frequency increases with the momentum and, correspondingly, the height of the peaks of the spectral function decrease.

The dissociation of quarkonium states inside the quark gluon plasma was studied before using lattice QCD [31–41], QCD sum rules [42–47], other previous holographic models [27, 48–50], effective field theories [53, 54] and potential models [55–58]. There are also experimental investigations as in ref. [59]. In particular, in [59] one finds a plot, on Figure 1, with a compilation of results for quarkonium dissociation temperatures from those different

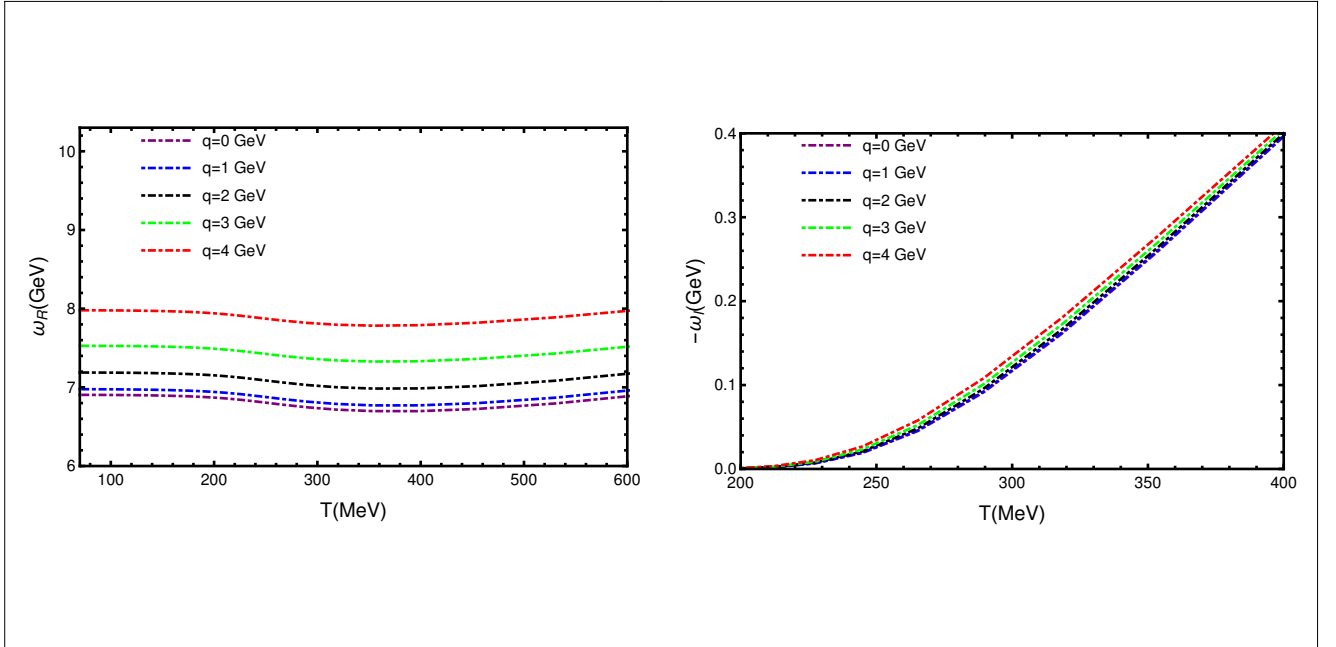


Figure 10. Numerical results for the quasinormal modes of the bottomonium in the transverse direction as function of the temperature.

approaches. The dissociation for charmonium at zero chemical potential happens for the ratio T/T_c in the range of 1.5 to 3.0. For bottomonium, the dissociation occurs in a range, that varies with the model, from $2 \leq T/T_c \leq 4$.

The effective holographic model presented here describes heavy mesons. That means: mesons made with quark flavors b and c . On the other hand, the quark gluon plasma is formed by the dissociation of the light quarks. A reasonable estimate for the critical temperature here is to use the value obtained in holographic soft wall model for the (light) rho meson[60]: $T_c \sim 190$ MeV. Then, the dissociation temperatures found here are consistent with the other predictions.

Regarding the effect of the motion relative to the plasma frame, reference [27] analysed mesons in motion in a plasma using the D7 brane model. An increase in the real part of the quasi-normal frequencies with the value of the momentum was found for both transverse and longitudinal motion. The same kind of result that we found here. For the imaginary part of the frequency, the authors of [27] found a decrease in the absolute value with the momentum for the longitudinal case, the same qualitative behavior found here. For the transverse case, the behavior that they found for the imaginary part of the frequencies depends on a parameter that characterizes the D7 brane embedding.

6 Appendix

We can understand better the effect of the introduction of the background $\phi(z)$ of eq. (2.4) in the holographic model by considering the hydrodynamical limit $\mathfrak{q} \ll 1$, $\mathfrak{w} \ll 1$. One considers the charge diffusion hydrodynamic dispersion relation, corresponding to the lowest quasinormal frequency [61]. Using the equation of motions for the vector field, together with appropriate boundary conditions give the dispersion law $\omega(q) = -Dq^2$ [61]. The charge diffusion constant can be obtained following the membrane paradigm as in ref. [62]

$$D = \frac{\sqrt{-g(z_h)}}{g_{eff}^2(z_h) \sqrt{-g_{tt}(z_h)g_{zz}(z_h)}} \int_0^{z_h} dz \frac{-g_{tt}(z)g_{zz}(z)}{\sqrt{-g(z)}} g_{eff}^2(z), \quad (6.1)$$

where g_{eff} is a z dependent coupling. Let's compute the diffusion constant for the AdS/CFT case, that corresponds to the strongly coupled $\mathcal{N} = 4$ SYM plasma. The metric of the gravity dual is given by eq. (2.11) and $g_{eff}^2 = g_5^2$. Then, one finds using (6.1)

$$D_{\mathcal{N}=4\text{SYM}} = \frac{1}{2\pi T}. \quad (6.2)$$

where the only parameter is the temperature. This is the result of refs. [61, 62].

In the case of the holographic model considered in this article the metric is the same but there is a z dependent coupling given by $g_{eff}^2 = e^{\phi(z)} g_5^2$. Therefore, the diffusion constant can be written as

$$D = \frac{e^{-\phi(z_h)}}{z_h} \int_0^{z_h} dz z e^{\phi(z)}. \quad (6.3)$$

For the dilaton profile (2.4) that includes a hyperbolic tangent term we could not find an analytic solution for D . The numerical solutions, for charmonium and bottomonium, were calculated and the results for the product $D2\pi T$ are shown in figure (11) as functions of the temperature divided by the mass of the first state. One can observe that, consistently, in the high temperature (conformal) limit the diffusion coefficient for both cases approaches the AdS/CFT value: $D = 1/2\pi T$. But for finite temperatures there is a non trivial dependence on T .

On the other hand, if one considers a dilaton profile similar to (2.4) but without the hyperbolic tangent: $\phi(z) = k^2 z^2 + Mz$, one finds an analytical solution that serves as an illustrative example of the effect of the background scalar field. The solution found using (6.1) is:

$$D = e^{-\frac{(2k^2 + M\pi T)^2}{4k^2\pi^2 T^2}} \pi T \left(2e^{M^2/4k^2} k \left(-1 + e^{\frac{(k^2 + M\pi T)}{\pi^2 T^2}} \right) + M\sqrt{\pi} \operatorname{Erfi} \left[\frac{M}{2k} \right] - M\sqrt{\pi} \operatorname{Erfi} \left[\frac{M}{2k} + \frac{k}{\pi T} \right] \right), \quad (6.4)$$

where $\operatorname{Erfi}(x) = -i \operatorname{Erf}(ix)$ is the imaginary error function. This analytical form shows us, for this simpler background, how the energy parameters k and M contribute to the charge

diffusion coefficient. This expression shows the non trivial dependence of D on the temperature for a holographic model, that contrasts with the trivial dependence of the conformal AdS/CFT case.

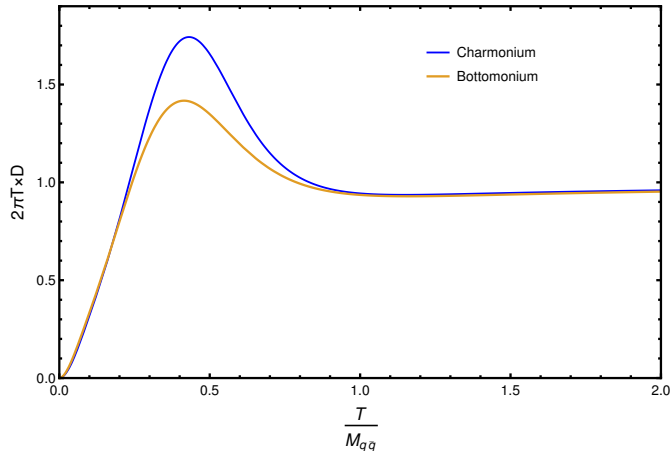


Figure 11. Numerical results for the charge diffusion coefficient of charmonium and bottomonium multiplied by $2\pi T$ as function of the temperature (rescaled by the mass of the first hadronic state).

Acknowledgments: N.B. is partially supported by CNPq (Brazil) under Grant No. 307641/2015-5 and L. F. Ferreira is supported by the National Council for Scientific and Technological Development CNPq.

References

- [1] T. Matsui and H. Satz, Phys. Lett. B **178**, 416 (1986). doi:10.1016/0370-2693(86)91404-8.
- [2] H. Satz, J. Phys. G **32**, R25 (2006) doi:10.1088/0954-3899/32/3/R01 [hep-ph/0512217].
- [3] N. R. F. Braga, M. A. Martin Contreras and S. Diles, Phys. Lett. B **763**, 203 (2016) [arXiv:1507.04708 [hep-th]].
- [4] N. R. F. Braga, M. A. Martin Contreras and S. Diles, Eur. Phys. J. C **76**, no. 11, 598 (2016) [arXiv:1604.08296 [hep-ph]].
- [5] N. R. F. Braga and L. F. Ferreira, Phys. Lett. B **773**, 313 (2017) [arXiv:1704.05038 [hep-ph]].
- [6] N. R. F. Braga, L. F. Ferreira and A. Vega, Phys. Lett. B **774**, 476 (2017) [arXiv:1709.05326 [hep-ph]].
- [7] N. R. F. Braga and L. F. Ferreira, Phys. Lett. B **783**, 186 (2018) [arXiv:1802.02084 [hep-ph]].
- [8] K. A. Olive *et al.* [Particle Data Group Collaboration], Chin. Phys. C **38**, 090001 (2014).
- [9] D. S. Hwang and G. H. Kim, Z. Phys. C **76**, 107 (1997) [hep-ph/9703364].
- [10] J. Polchinski and M. J. Strassler, Phys. Rev. Lett. **88**, 031601 (2002) [arXiv:hep-th/0109174].
- [11] H. Boschi-Filho and N. R. F. Braga, Eur. Phys. J. C **32**, 529 (2004) [arXiv:hep-th/0209080].

- [12] H. Boschi-Filho and N. R. F. Braga, *JHEP* **0305**, 009 (2003) [arXiv:hep-th/0212207].
- [13] A. Karch, E. Katz, D. T. Son and M. A. Stephanov, *Phys. Rev. D* **74**, 015005 (2006) doi:10.1103/PhysRevD.74.015005 [hep-ph/0602229].
- [14] G. T. Horowitz and V. E. Hubeny, *Phys. Rev. D* **62**, 024027 (2000) [hep-th/9909056].
- [15] D. T. Son and A. O. Starinets, *JHEP* **0209**, 042 (2002) doi:10.1088/1126-6708/2002/09/042 [hep-th/0205051].
- [16] A. Nunez and A. O. Starinets, *Phys. Rev. D* **67**, 124013 (2003) [hep-th/0302026].
- [17] P. K. Kovtun and A. O. Starinets, *Phys. Rev. D* **72**, 086009 (2005) doi:10.1103/PhysRevD.72.086009 [hep-th/0506184].
- [18] A. S. Miranda and V. T. Zanchin, *Phys. Rev. D* **73**, 064034 (2006) [gr-qc/0510066].
- [19] C. Hoyos-Badajoz, K. Landsteiner and S. Montero, *JHEP* **0704**, 031 (2007) [hep-th/0612169].
- [20] E. Berti, V. Cardoso and A. O. Starinets, *Class. Quant. Grav.* **26**, 163001 (2009) [arXiv:0905.2975 [gr-qc]].
- [21] J. Morgan, V. Cardoso, A. S. Miranda, C. Molina and V. T. Zanchin, *Phys. Rev. D* **80**, 024024 (2009) [arXiv:0906.0064 [hep-th]].
- [22] A. S. Miranda, C. A. Ballon Bayona, H. Boschi-Filho and N. R. F. Braga, *JHEP* **0911**, 119 (2009) [arXiv:0909.1790 [hep-th]].
- [23] R. A. Konoplya and A. Zhidenko, *Rev. Mod. Phys.* **83**, 793 (2011) [arXiv:1102.4014 [gr-qc]].
- [24] L. A. H. Mamani, A. S. Miranda, H. Boschi-Filho and N. R. F. Braga, *JHEP* **1403**, 058 (2014) [arXiv:1312.3815 [hep-th]].
- [25] L. A. H. Mamani, J. Morgan, A. S. Miranda and V. T. Zanchin, *Phys. Rev. D* **98**, no. 2, 026006 (2018) [arXiv:1804.01544 [gr-qc]].
- [26] M. Kaminski, *Fortsch. Phys.* **57**, 3 (2009) [arXiv:0808.1114 [hep-th]].
- [27] M. Kaminski, K. Landsteiner, F. Pena-Benitez, J. Erdmenger, C. Greubel and P. Kerner, *JHEP* **1003**, 117 (2010) [arXiv:0911.3544 [hep-th]].
- [28] I. Amado, M. Kaminski and K. Landsteiner, *JHEP* **0905**, 021 (2009) doi:10.1088/1126-6708/2009/05/021 [arXiv:0903.2209 [hep-th]].
- [29] M. Kaminski, K. Landsteiner, J. Mas, J. P. Shock and J. Tarrío, *JHEP* **1002**, 021 (2010) doi:10.1007/JHEP02(2010)021 [arXiv:0911.3610 [hep-th]].
- [30] S. Janiszewski and M. Kaminski, *Phys. Rev. D* **93**, no. 2, 025006 (2016) [arXiv:1508.06993 [hep-th]].
- [31] T. Umeda, R. Katayama, O. Miyamura and H. Matsufuru, *Int. J. Mod. Phys. A* **16**, 2215 (2001) doi:10.1142/S0217751X0100355X [hep-lat/0011085].
- [32] M. Asakawa and T. Hatsuda, *Phys. Rev. Lett.* **92**, 012001 (2004) doi:10.1103/PhysRevLett.92.012001 [hep-lat/0308034].
- [33] S. Datta, F. Karsch, P. Petreczky and I. Wetzorke, *Phys. Rev. D* **69**, 094507 (2004) doi:10.1103/PhysRevD.69.094507 [hep-lat/0312037].

- [34] A. Jakovac, P. Petreczky, K. Petrov and A. Velytsky, Phys. Rev. D **75**, 014506 (2007) doi:10.1103/PhysRevD.75.014506 [hep-lat/0611017].
- [35] G. Aarts, C. Allton, M. B. Oktay, M. Peardon and J. I. Skullerud, Phys. Rev. D **76**, 094513 (2007) doi:10.1103/PhysRevD.76.094513 [arXiv:0705.2198 [hep-lat]].
- [36] A. Rothkopf, T. Hatsuda and S. Sasaki, Phys. Rev. Lett. **108**, 162001 (2012) doi:10.1103/PhysRevLett.108.162001 [arXiv:1108.1579 [hep-lat]].
- [37] G. Aarts, C. Allton, S. Kim, M. P. Lombardo, M. B. Oktay, S. M. Ryan, D. K. Sinclair and J. I. Skullerud, JHEP **1111**, 103 (2011) doi:10.1007/JHEP11(2011)103 [arXiv:1109.4496 [hep-lat]].
- [38] G. Aarts, S. Kim, M. P. Lombardo, M. B. Oktay, S. M. Ryan, D. K. Sinclair and J.-I. Skullerud, Phys. Rev. Lett. **106**, 061602 (2011) doi:10.1103/PhysRevLett.106.061602 [arXiv:1010.3725 [hep-lat]].
- [39] G. Aarts, C. Allton, S. Kim, M. P. Lombardo, M. B. Oktay, S. M. Ryan, D. K. Sinclair and J. I. Skullerud, JHEP **1303**, 084 (2013) doi:10.1007/JHEP03(2013)084 [arXiv:1210.2903 [hep-lat]].
- [40] G. Aarts, C. Allton, S. Kim, M. P. Lombardo, S. M. Ryan and J.-I. Skullerud, JHEP **1312**, 064 (2013) doi:10.1007/JHEP12(2013)064 [arXiv:1310.5467 [hep-lat]].
- [41] F. Karsch, E. Laermann, S. Mukherjee and P. Petreczky, Phys. Rev. D **85**, 114501 (2012) doi:10.1103/PhysRevD.85.114501 [arXiv:1203.3770 [hep-lat]].
- [42] K. Morita and S. H. Lee, Phys. Rev. Lett. **100** (2008) 022301 doi:10.1103/PhysRevLett.100.022301 [arXiv:0704.2021 [nucl-th]].
- [43] K. Morita and S. H. Lee, Phys. Rev. C **77**, 064904 (2008) doi:10.1103/PhysRevC.77.064904 [arXiv:0711.3998 [hep-ph]].
- [44] Y. H. Song, S. H. Lee and K. Morita, Phys. Rev. C **79**, 014907 (2009) doi:10.1103/PhysRevC.79.014907 [arXiv:0808.1153 [hep-ph]].
- [45] K. Morita and S. H. Lee, Phys. Rev. D **82**, 054008 (2010) doi:10.1103/PhysRevD.82.054008 [arXiv:0908.2856 [hep-ph]].
- [46] P. Gubler, K. Morita and M. Oka, Phys. Rev. Lett. **107**, 092003 (2011) doi:10.1103/PhysRevLett.107.092003 [arXiv:1104.4436 [hep-ph]].
- [47] K. Suzuki, P. Gubler, K. Morita and M. Oka, Nucl. Phys. A **897**, 28 (2013) doi:10.1016/j.nuclphysa.2012.09.011 [arXiv:1204.1173 [hep-ph]].
- [48] Y. Kim, J. P. Lee and S. H. Lee, Phys. Rev. D **75**, 114008 (2007) doi:10.1103/PhysRevD.75.114008 [hep-ph/0703172 [HEP-PH]].
- [49] M. Fujita, K. Fukushima, T. Misumi and M. Murata, Phys. Rev. D **80**, 035001 (2009) doi:10.1103/PhysRevD.80.035001 [arXiv:0903.2316 [hep-ph]].
- [50] J. Noronha and A. Dumitru, Phys. Rev. Lett. **103**, 152304 (2009) doi:10.1103/PhysRevLett.103.152304 [arXiv:0907.3062 [hep-ph]].
- [51] M. Laine, JHEP **0705**, 028 (2007) doi:10.1088/1126-6708/2007/05/028 [arXiv:0704.1720 [hep-ph]].

- [52] C. Y. Wong, Phys. Rev. C **72**, 034906 (2005) doi:10.1103/PhysRevC.72.034906 [hep-ph/0408020].
- [53] N. Brambilla, J. Ghiglieri, A. Vairo and P. Petreczky, Phys. Rev. D **78**, 014017 (2008) doi:10.1103/PhysRevD.78.014017 [arXiv:0804.0993 [hep-ph]].
- [54] S. Digal, O. Kaczmarek, F. Karsch and H. Satz, Eur. Phys. J. C **43**, 71 (2005) doi:10.1140/epjc/s2005-02309-7 [hep-ph/0505193].
- [55] W. M. Alberico, A. Beraudo, A. De Pace and A. Molinari, Phys. Rev. D **72**, 114011 (2005) doi:10.1103/PhysRevD.72.114011 [hep-ph/0507084].
- [56] A. Mocsy and P. Petreczky, Phys. Rev. D **77**, 014501 (2008) doi:10.1103/PhysRevD.77.014501 [arXiv:0705.2559 [hep-ph]].
- [57] A. Mocsy and P. Petreczky, Phys. Rev. Lett. **99**, 211602 (2007) doi:10.1103/PhysRevLett.99.211602 [arXiv:0706.2183 [hep-ph]].
- [58] P. Petreczky, C. Miao and A. Mocsy, Nucl. Phys. A **855**, 125 (2011) doi:10.1016/j.nuclphysa.2011.02.028 [arXiv:1012.4433 [hep-ph]].
- [59] A. Adare *et al.* [PHENIX Collaboration], Phys. Rev. C **91**, no. 2, 024913 (2015) doi:10.1103/PhysRevC.91.024913 [arXiv:1404.2246 [nucl-ex]].
- [60] C. A. Ballon Bayona, H. Boschi-Filho, N. R. F. Braga and L. A. Pando Zayas, Phys. Rev. D **77**, 046002 (2008) doi:10.1103/PhysRevD.77.046002 [arXiv:0705.1529 [hep-th]].
- [61] G. Policastro, D. T. Son and A. O. Starinets, JHEP **0209**, 043 (2002) doi:10.1088/1126-6708/2002/09/043 [hep-th/0205052].
- [62] P. Kovtun, D. T. Son and A. O. Starinets, JHEP **0310**, 064 (2003) doi:10.1088/1126-6708/2003/10/064 [hep-th/0309213].